Defence Research Establishment Pacific
Centre de recherches pour la défense pacifique

DEFENCE RESEARCH ESTABLISHMENT PACIFIC

CFB Esquimalt, FMO Victoria, B.C. VOS 1BO

Technical Memorandum 88-26

ANALYSIS OF SIDE-SCAN SONAR IMAGES OF A HIGH-REFLECTIVITY TARGET

by

J.M. Preston, R.H. Poeckert,
M.G. Tribes, and W.H. Vogel

Electromagnetics Section
Physics Research Division
Defence Research Establishment Pacific

December 1988

Approved by:

J. Garrett

CHIEF

Research and Development Branch
Department of National Defence

Canada

91-00064/

ABSTRACT

An investigation of the image produced by a commercial side-scan sonar operating against moored reflectors is reported. This study of reflections from triangular corner cubes showed that energy broadcast and received at angles of up to 30^{o} can appear on the image of high reflectivity targets, even with sonars of nominal beamwidths of less than 1^{o}. This unusual image was found to be consistent with the beam pattern of the transducer. An effect of towfish yaw could also be seen in the image studied.

INTRODUCTION

Side-scan sonars deployed on towfish are a valued tool for imaging the sea bottom. Even though the concepts involved are straightforward and considerable experience has been gained, there is still a need for basic studies in some areas, such as the practical effects of sidelobes and the effects of towfish attitude on the image. This Memorandum describes some recent observations in both these areas.

The images analyzed here are of corner-cube reflectors, which give a very strong reflection which is visible over a wide range of angles. The internal structure of this reflection can be studied to investigate the beam pattern. It also was possible, in this case, to see an effect of towfish yaw.

PROCEDURE

Comparative trials of commercial side-scan sonars were carried out in July 1986. Various targets had been placed on, or moored close to, a smooth bottom near Esquimault. Included among these targets were six pairs of corner reflectors, and it is the reflections from these which are the subject of this study. The towing vessel was the CFAV Endeavour, which towed the sonar towfish past the targets at speeds of typically 2 m/s along parallel lines spaced 40 m apart. The vessel was navigated with a Racal Microfix microwave positioning system using the Precise Integrated Navigation System (PINS) manufactured by Offshore Systems Ltd., Vancouver. The ship-towfish distance and the towfish depth were recorded continually by means of a Range-Depth Unit manufactured by Mesotech Ltd., Vancouver. The bearing from the ship to the towfish was estimated by an iterative procedure which located the towfish directly beneath a point on the surface which was at the correct range and on the line between the current ship position and the surface point directly above the previous towfish position. Further

above the previous towfish position. Further details are available in Reference 1, which describes a similar Exercise done in 1987. Reference 2 is a detailed analysis of the inaccuracies inherent in this iterative procedure.

The corner cubes each consisted of three square aluminium plates, 30 cm on each side, slotted and joined along their diagonals. Each corner cube therefore had eight triangular reflectors 21.2 cm on a side, as shown on Figure 1. They were deployed, in six pairs, on a line between an anchor and a float, at a height of about 4 m above the bottom. Each corner cube was oriented with one triangular reflector vertically upward and one downward, as if it were resting on a horizontal surface. The second of each

Figure 1. Corner cubes as built for this trial. The material was 1/4" aluminium plate. The float was an 11" sphere.

pair was rotated 35° with respect to the first about their common mooring line.

The sonar data from the passes analyzed in this study were obtained from a Klein 500 towfish on the 50-m range setting. The analog sonar data were recorded on a Klein 531T wet-paper chart recorder and also on a seven-track tape recorder. Back in the laboratory, the data were digitized with 16 bits accuracy and a sampling rate of 50 kHz. The portion of data which contained the selected hyperbolae was processed with the Magnetics Interactive Command (MAGIC) package developed at DREP, which was also used to generate the overlay. The pixel size was calculated as follows: there were 15 pings/s on each side and thus 1667 points per ping at 50-kHz total sampling rate and thus 50 m/1667 = 0.030 m cross-track resolution; at 2 m/s and 15 pings/s the along-track resolution was 0.13 m.

RESULTS AND ANALYSIS

Corner-Cube Reflectors

Triangular corner-cube reflectors consist of three square plates joined along their diagonals at right angles, as shown in Figure 1. The resulting structure has eight open triangular faces, with the border between faces being the hypotenuse of an isosceles right-angled triangle whose vertex is at the common centre of the plates. Each trihedral structure has the property that any ray incident into a triangular face will, for a wide range of angles of incidence, be reflected back upon itself after reflection from all three plates. Directional reflection results in a much larger target strength than an isotropic scatterer such as a sphere.

The theory of the effective reflecting area of corner reflectors is a calculation of the overlap area of the entrance and exit pupils. The entrance pupil is the corner as seen from the direction of the incident beam; the exit pupil is the entrance pupil reflected about the origin, since

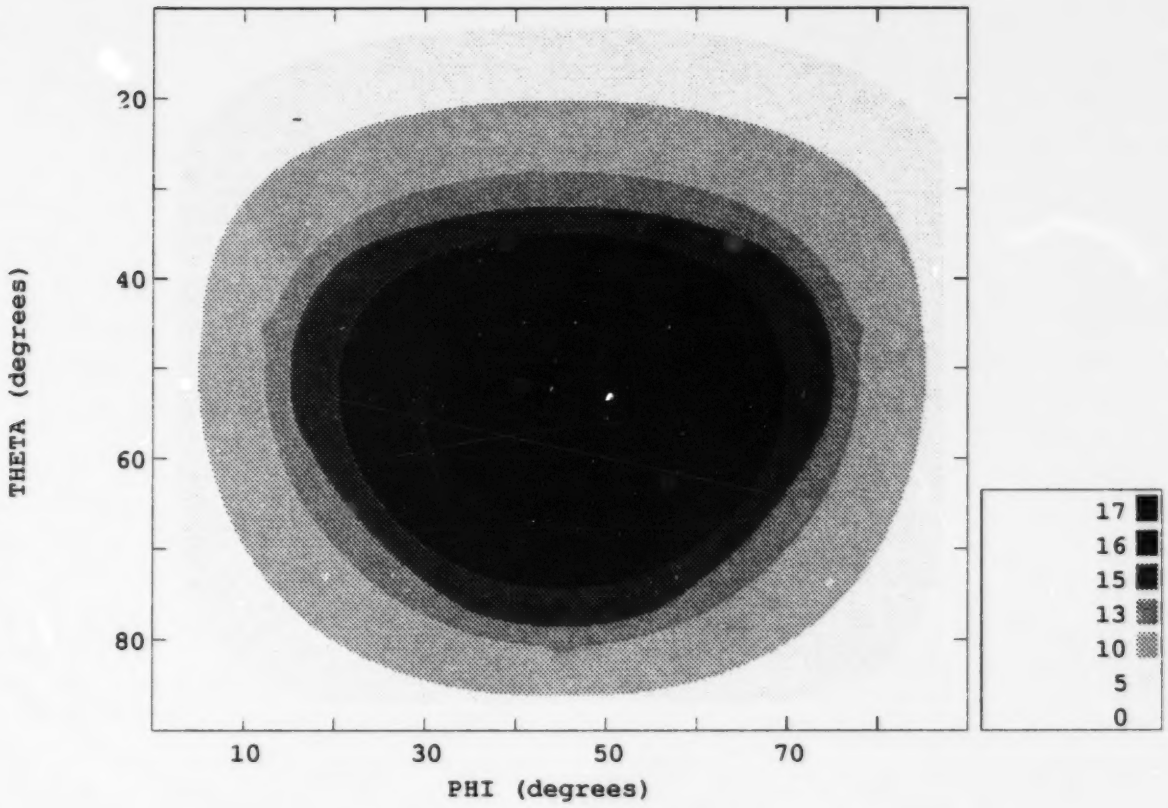

Figure 2. Calculated target strength of a triangular corner reflector with three equal sides of 21.2 cm (hypotenuse 30 cm) for a sonar at 340 kHz. The target strengths are in dB referenced to 1 m. The angle from one vertex of the reflector is θ, and ϕ is the angle in the plane perpendicular to that vertex.

that is the consequence of the three reflections. The overlap area can be four- or six-sided. The original reference appears to be by Spencer (3), and we found no more recent paper (e.g. 4) nearly as complete. The tabulation by Urick (5) includes Spencer's approximation for the central maximum.

Spencer's results are in terms of the angles between the incident vectors, the axis of the corner, and the angle to the nearest vertex. More convenient for the present purposes is the target strength as a function of the angles of a spherical coordinate system. This is less general, since

one vertex has to be selected as the axis from which θ is measured, while ϕ is the angle in the other plane. Plots of target strength as a function of (θ,ϕ) do, however, allow the target strength seen by the sonar to be pictured, and such a plot is given as Figure 2. It was calculated from a FORTRAN program based on the equations given by Spencer. Note that the target strength depends on the sonar frequency - a frequency of 430 kHz (6) was used here. The plot shows that the target strength is indeed high, +17.5 dB reference 1 m, and falls only 2 dB out to 22^{o} in any direction (since the scale is the same on both axes, angular variations can be read in any direction).

Because the target strength of a corner reflector does fall off sharply at more than about 35^{o} from the axis, the twelve corner cubes were mounted in pairs, one above the other, with one member of each pair rotated about 35^{o} from the other. While this made the return much less dependant on aspect, it appears to have caused an interference effect which will be discussed later.

The consequence of departures from perpendicularity in construction of the reflectors is that the beam is reflected at an angle twice the sum of the errors (7). Care was taken in the construction to reduce this effect to less than 1^{o}.

Horizontal Beam Pattern of the Klein 500 Transducer

In preparation for the analysis of these images, a program was written to calculate the beam pattern from a long thin transducer. The Rayleigh distance, which is one criterion for separating the near-field from the far-field, is L^2/λ, where L is the length of the transducer and λ the wavelength. Since typical ranges to these reflectors are less than the Rayleigh distance, the beam pattern was calculated into the near field, in fact to within 10 L of the transducer face. A second motivation for this calculation was that some authors (8) hold that the near-field to far-field transition occurs near $L^2/4\lambda$. This distinction is crucial for short range, high resolution sonar, and so plots were produced which include the pressure distribution in the transition zone.

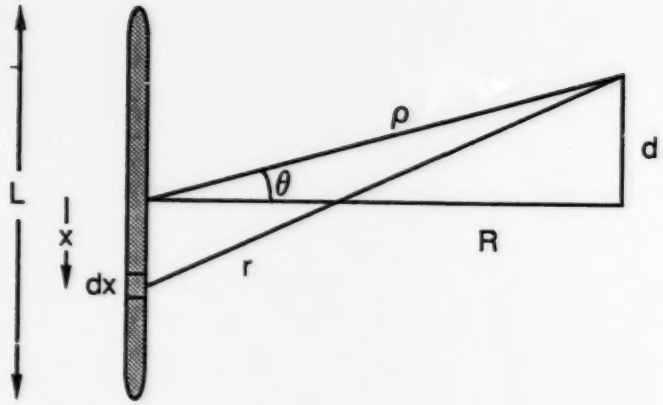

Figure 3. To calculate the beam pattern from a thin transducer of length L at field point (ρ,θ), an integral along the length is done, with the distance r as the distance between the field point and the transmitting element.

The aim of the calculation, then, was to calculate the amplitude, A, of the pressure wave from a linear transducer. Figure 3 shows the geometry. We start with the general expression for the pressure in the vicinity of a baffled source (Ref. 8, Chap. 8)

$$P(\rho,t) = \frac{j\rho_o cQ}{\lambda r} e^{j(\omega t-kr)} \qquad (1)$$

where $\rho_o c$ is the characteristic impedance, Q the source strength, ω the frequency, and $k=2\pi/\lambda$. Considering the transducer to be made up of a large number of rectangles of the same width as the transducer, w, and length dx, gives $dQ = U_o w dx$, where U_o is the amplitude of the vibration of the element. The actual pressure is then

$$P(\rho,\theta,t) = \frac{j\rho_o cU_o w}{\lambda} \int_{-L/2}^{L/2} \frac{1}{r} e^{j(\omega t-kr)}\, dx \qquad (2)$$

From Figure 3

$$r^2 = \rho^2 + 2\rho x \sin\theta + x^2 \tag{3}$$

so we can define a function F as

$$r = \rho(1 - F(x/\rho,\theta)) \tag{4}$$

that is

$$F(\chi,\theta) = 1 - \left[1 + 2\,\chi\,\sin\theta + \chi^2 \right]^{1/2} \tag{5}$$

giving

$$P(\rho,\theta,t) = \frac{j\rho_o c U_o w}{\lambda}\; e^{j(\omega t - k\rho)} \int_{-L/2}^{L/2} \frac{e^{jk\rho F(x/\rho,\theta)}}{(\rho^2 + 2\rho x\sin\theta + x^2)^{1/2}}\; dx \tag{6}$$

The purpose of defining F was to remove the factor $e^{j(\omega t - k\rho)}$ from the integrand so as to obtain an expression for the amplitude of the pressure, namely the product of the integral and the leading constants. The desired final expression is the amplitude, $A(\rho,\theta)$

$$A(\rho,\theta) = \frac{j\rho_o c U_o w}{\lambda} \int_{-L/2}^{L/2} \frac{e^{jk\rho F(x/\rho,\theta)}}{(\rho^2 + 2\rho x\sin\theta + x^2)^{1/2}}\; dx \tag{7}$$

This form for the amplitude was used in the analysis of the reflections from the corner cubes.

To gain an appreciation for the beam pattern itself, Equation 7 was used to write an expression for A'(R,d), where A' is a normalized amplitude and R and d are as in Figure 3. Evaluating this expression gave the contour plot of Figure 4, for the Klein 500, which has a transducer length of 432 mm and a wavelength of 3.4 mm (for the actual operating frequency of 430 kHz). To understand this plot, it is important to realize that both R and d have been made unitless by division by λ, and that each

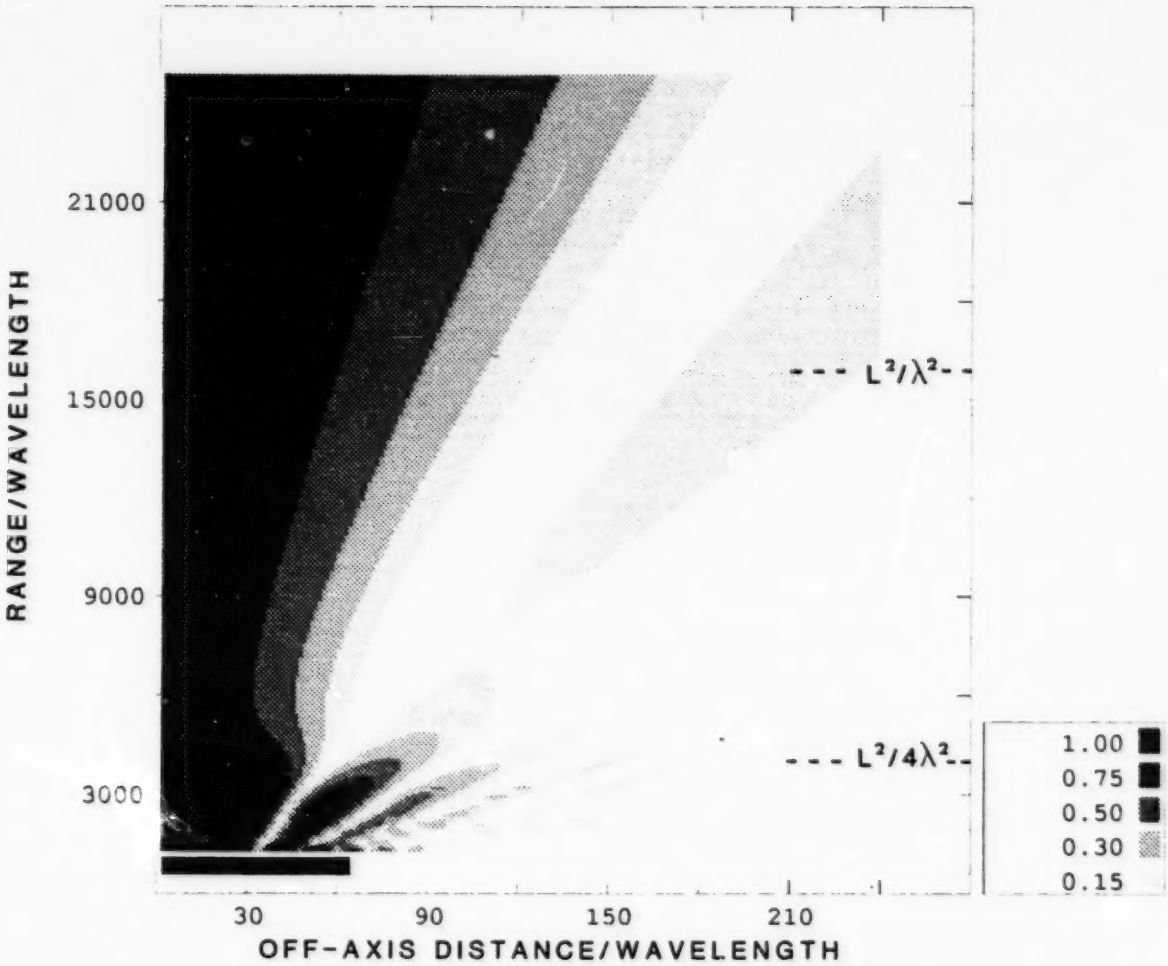

Figure 4. Calculated amplitude distribution of a Klein "500 kHz" transducer operating at 430 kHz. The range and the off-axis distance have both been divided by the wavelength before plotting, and the axes are to quite different scales. The amplitudes at each range have been normalized to unity at zero distance off axis.

line of constant R/λ has been normalized to unity at d=0. Furthermore, note the vastly different scales on the two axes.

This plot clearly shows the different beam patterns in the near and far fields, and the neck in amplitude near the transition region. Because the axes have been normalized to the wavelength, this pattern applies to all long thin transducers. There is, of course, no sharp

border between the near and far fields, but it is clear that the Rayleigh distance, L^2/λ, is in a region with far-field characteristics, while $L^2/4\lambda$ is in the near field. The Rayleigh distance is important, though, in a common simple model of the beam pattern, namely a slab of width equal to the length of the transducer out to the Rayleigh distance, with spreading at larger ranges at the angle $\sin^{-1}(\lambda/L)$. It can be seen that L^2/λ is an appropriate range for the transition in this model. For the Klein "500", the Rayleigh distance is 54 m.

A comparison with observed beam patterns is possible, due to some work from ARE Portland (6). Figures 65 and 66 of Reference 6 are transmitter polar output power of the Klein 500 in the horizontal plane at 75 m. Entering Figure 4 at R/λ = 17200 (75 m/3.4 mm) gives 75% of axis amplitude at off-axis distance/wavelength of 58, thus 0.19°, 50% at 0.29°, 30% at 0.37°, and 15% at 0.43°. Translating these fractions into power in dB gives points which reproduce the observations shown in the plot in Reference 6. Plot 105 of that Reference gives output power at a range of 7.1 m , which is in a complex portion of the near field (R/λ = 2060 on Figure 2). These observations do not reproduce the rapid theoretical variations calculated here, but agree well within a smoothed plot. Thus observation and theory agree well.

Sonar Records of Targets of High Reflectivity

The combination of a target of very high reflectivity and a sonar transducer with finite side lobes produces a hyperbolic image of the object on the sonar record. This image arises because enough of the off-main-beam sonar power is reflected to cause darkening of the sonar record. A hyperbolic shape will be found whenever the towfish follows a straight line, as shown in Figure 5. At each position along the trajectory the reflection from the corner cube appears on the sonar record at a distance corresponding to the distance between the towfish at that location and the corner cube. The equation of the sonar trace is

$$\rho^2 - (vt)^2 = R^2 \qquad (8)$$

where ρ is the apparent slant range to the reflector at time t, as in Figure 3, and v is the towfish speed. The constant R is the towfish-reflector distance when the reflector is abeam of the towfish, as in Figure 3. Note that ρ=R at the origin of time, that ρ is at its minimum at this ping, and that the peak intensity occurs with the reflector abeam, that is, at the same time.

For Equation 8 to apply, the towfish must have followed a straight trajectory at constant speed and with no yaw. If a straight trajectory is assumed, but a yaw angle ϕ is included, the equation of the sonar trace is

$$\rho^2 - (vt - R \sin\phi)^2 = R^2\cos^2\phi \qquad (9)$$

Note that the maximum intensity still occurs at t=0, since when ρ=R the reflector is abeam of the towfish, but that this point is no longer the part of the trace at the minimum slant range.

The sonar record which showed the clearest hyperbolic patterns was selected for analysis, and appears as the green and blue portions of Figure 6. Four of the six hyperbolae are clearly visible, as is the surface return. The other two hyperbolae are very similar in appearance and were not considered further. The cross-track distances shown are slant ranges. It would, in fact, have been inappropriate to use horizontal ranges, because all the analysis described below considers only the plane defined by the towfish trajectory and the reflector. The along-track distance is from an arbitrary zero.

Equations 7 and 9 allow the theoretical hyperbolic pattern to be calculated. In the computer program it was convenient to consider time to be the independent variable and to compute, for a series of times, the bearing and range from the towfish to the reflector and thus the intensity and position of the corresponding highlight on the sonar record. The period between time points was set equal to the period between pings, to best mimic the acquisition of the sonar record. This was done for each hyperbola, using the actual values of slant range to the reflector when the towfish was

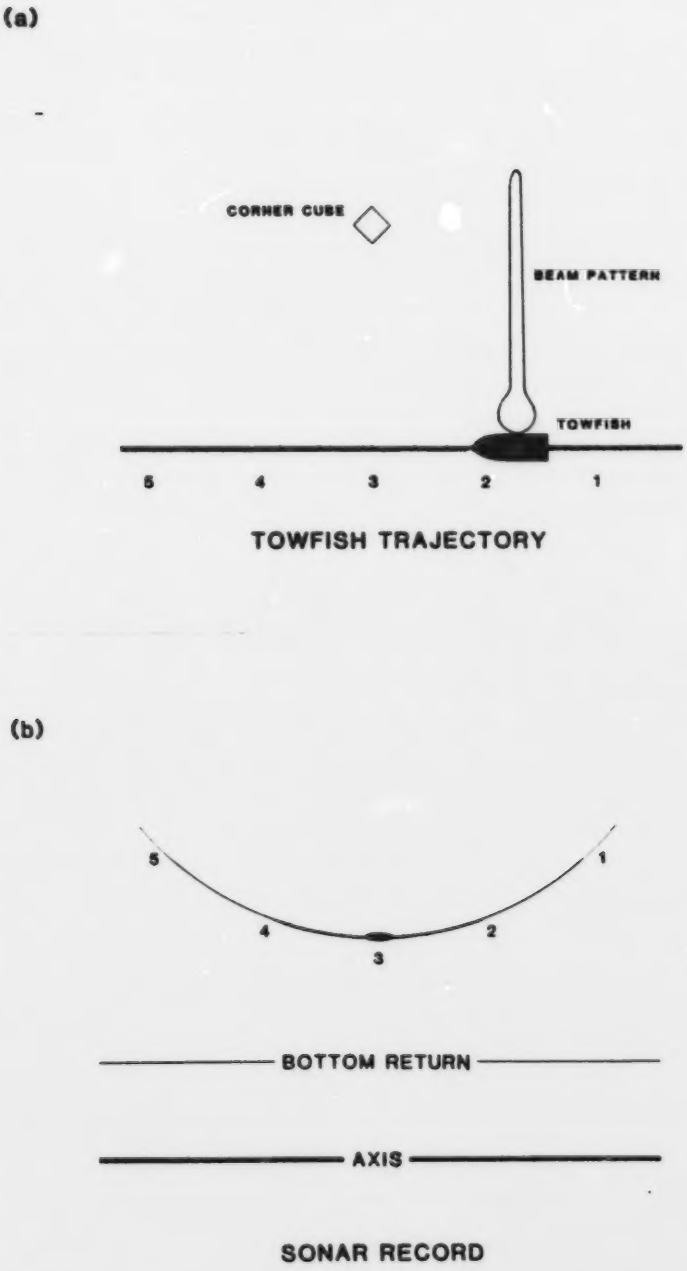

Figure 5. When a towfish passes a target of high reflectivity with the geometry shown on part a, the resulting sonar record contains hyperbolae, as shown in part b, because of the off-axis acoustic energy.

abeam, R, as measured from the sonar records (34.0, 34.6, 35.3, and 37.3 m). There remained two adjustable variables, the along-track coordinate of the vertex of each hyperbola, and the yaw, which would be expected to be constant for the set of four hyperbolae. The four along-track coordinates were chosen to give the best fit in each case, and it was found that a yaw angle, ϕ, of -5^{o} gave the best agreement with observation. Figure 6 shows the calculated hyperbolae (red and yellow) overlayed on the observed hyperbolae (blue and green). In both images only the strongest returns are plotted, and thus the bottom return is largely missing (although a strong surface return can be seen), and portions of the hyperbolae which consist of reduced intensities appear as white.

The good agreement between the locations of the arms of the sonar records and the overlays shows that the towfish was travelling at a constant velocity and with constant yaw throughout this period. The constant yaw also produces the consistent agreement in the location of the maximum return, which is certainly not at the minimum range, as discussed above. The separation between the theoretical and observed arms of the uppermost hyperbola, the last one imaged, suggests that the towfish decelerated during this part of the pass. Unfortunately the navigational information is not precise enough to verify this hypothesis.

The theoretical hyperbolae do not show the intensity variation evident in the sonar records. The along-track spacing between maxima in the sonar records is typically 5 m, while the theoretical spacing is 0.4 m near the vertex and 1.2 m near the extremes of the arms. The minima of the theoretical pattern appear in Figure 6 as gaps between the coloured areas. They can be seen readily in the arms but not at the vertex for two reasons: the wider spacing at the extremes, and the difference in the along- and across-track scales which compresses each plot near the vertex. The discrepancy in the spacing of the maxima is discussed in the next Section.

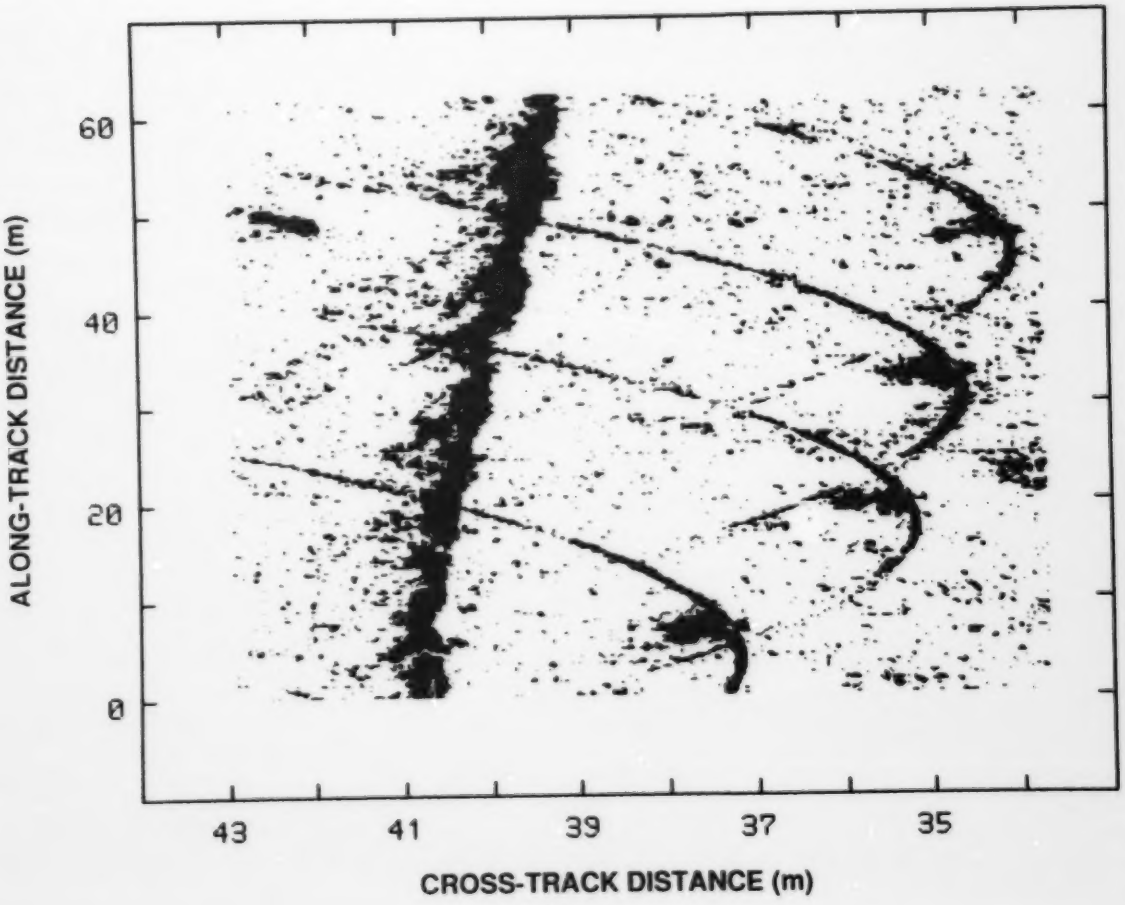

Figure 6. Extract from a sonar record of a Klein 500 kHz towfish showing, in green and blue, (deep blue › light blue › green) hyperbolic reflections from four pairs of corner cubes at the slant ranges indicated. The along-track distance is from an arbitrary zero. Overlaid are theoretical results in yellow and red (yellow › purple › red) for the corner cubes and sonar used in this trial at the ranges shown, with towfish yaw (same for all four) and along-track distance adjusted for best fit.

Intensity Distribution along a Hyperbola

The resolution of the sonar is inadequate to resolve maxima and minima due to the beam pattern close to the vertex of an hyperbola. Near the vertex, the return is spread along the along-track direction where the nominal resolution is about 0.2 m, insufficient to resolve a sinusoid of spatial period 0.4 m. Further along the hyperbola the spacing compares favourably with the cross-track resolution of about 0.03 m, and in some cases the intensities of the theoretical and observed hyperbolae agree well. In general, though, these sonar returns are not much above the noise level of the image (most of which is volume reverberation, plus the obvious surface return) and thus the intensity pattern cannot be discerned.

Maxima along the arms of the observed hyperbolae can indeed be discerned, however, and they are much too widely spaced to be due to the theoretical beam pattern. The experimental observation from this sonar record is that up to four maxima can be seen in each arm of each hyperbola. The angular spacings are shown in Figure 7, and average 11°, ignoring the lesser maxima. Other sonar records showing these corner cubes and taken with the same towfish show mean angular spacings between maxima of 2° and 9° in two different passes while no maxima are visible in two other passes.

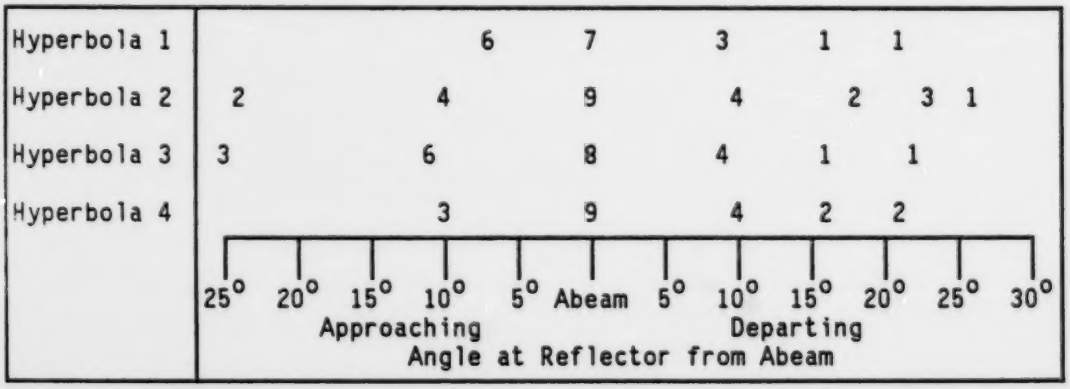
Hyperbola 1
6 7 3 1 1
Hyperbola 2
2 4 9 4 2 3 1
Hyperbola 3
3 6 8 4 1 1
Hyperbola 4
3 9 4 2 2
25° 20° 15° 10° 5° Abeam 5° 10° 15° 20° 25° 30°
Approaching
Departing
Angle at Reflector from Abeam

Figure 7. Chart illustrating the angular separation between the maxima observed in the hyperbolae appearing in Figure 6. The angle shown is the angle at the reflector between the position at which the reflector is abeam of the towfish and the towfish position which produced the maximum. Values are the peak intensity on a decibel scale adjusted to give values from 1-9.

Angular spacings of the order of 11° are too small to be due to the target strength of the corner cubes, as can be seen from Figure 2. A possible, although apparently incorrect, explanation for the observed maxima is that the beam pattern contains these maxima due to non-ideal behaviour of the transducer or some type of reflective interference in the body. The transducer could perhaps be responding to the piezoelectric driving force in short regions, resulting in widely-spaced maxima, either alone or as a modulation of the ideal beam pattern. Such explanations do not appear to apply to these observations because they would cause the same angular separations in all sonar records of a high reflectivity target, which is contrary to observation.

The only model which appears to explain the observations is interference between the returns from the two corner cubes of each pair. One property of these trihedral reflectors is that all retro-reflecting paths travel the same path length, thus the pair of corner cubes constitute a pair of coherent sources. They would not be equally intense sources, because their orientations differed by about 35°, thus minima rather than nulls would occur. Typically, working with Figure 2, the trajectory of the towfish would be specified as a line at $\theta \simeq 41^{\circ}$ as ϕ varies from 0° to 90° (upward-looking corner), followed by a quicker traverse at $\theta \simeq 30^{\circ}$ as ϕ varies from 0° to 90° (downward-looking corner). An offset of 35° in ϕ would thus result in two sources of comparable intensity.

Figure 8 is the calculated interference pattern in the vertical plane containing the towfish trajectory for a pair of coherent sources, separated vertically by the distance used in this deployment, 0.3 m (only one of the symmetrical quadrants was plotted). In the ideal case, without currents, the towfish would pass through this pattern at a vertical distance of about 3 m, since the towfish is typically 7 m above the bottom, the reflectors about 4 m. Maxima separated by about 25 m along-track (35° at 35-m range) would be seen. However it is known that tidal currents were present (and were the probable cause of the observed towfish yaw). In a current the corner cubes would lean. The component of lean perpendicular to the towfish trajectory is equivalent to a change in the vertical separation, while the effect of the component of lean parallel to the

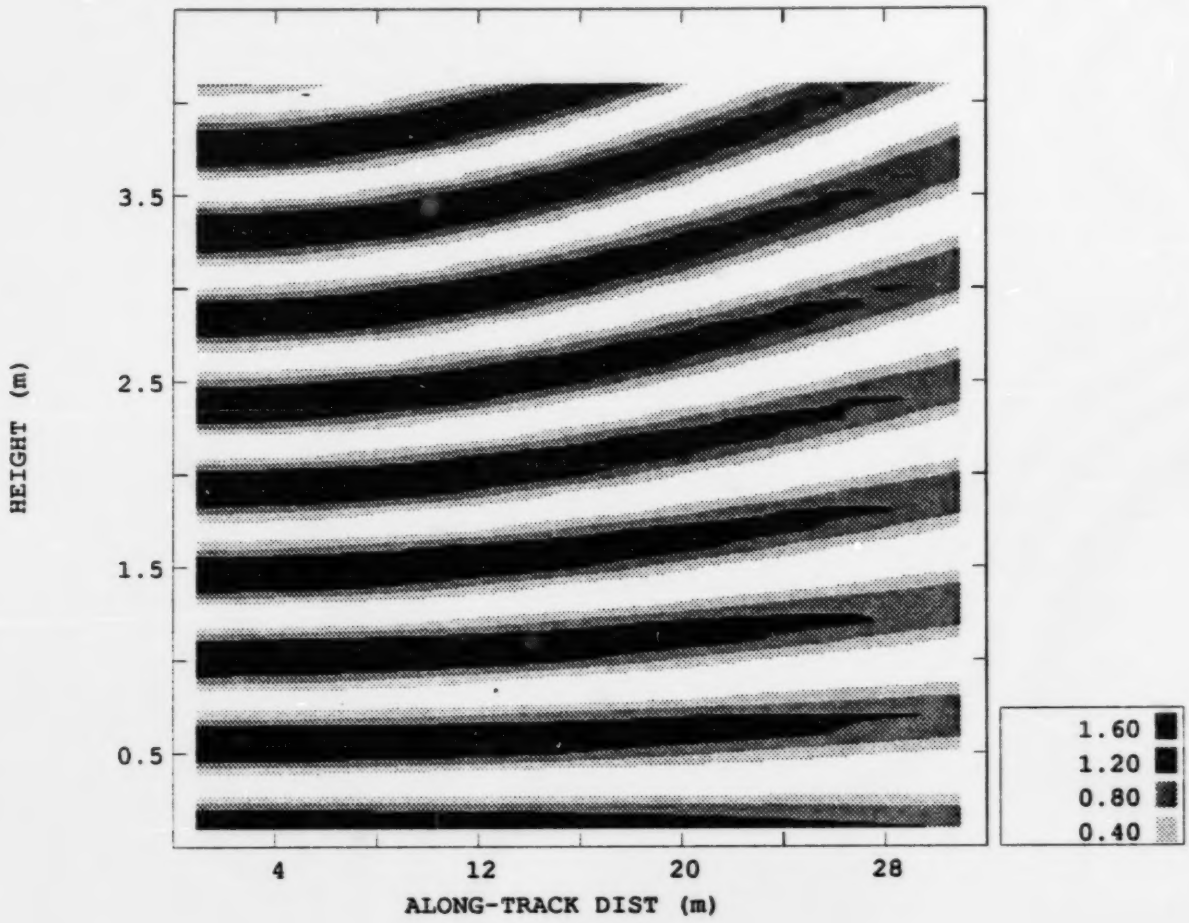

Figure 8. Amplitude distribution in the vertical plane containing the towfish trajectory due to the interference between two equal sources separated vertically by 0.3 m at a distance of 35 m. Each source is of unity amplitude, so the range of values shown is from 0 to 2.

trajectory is to rotate the interference pattern by that angle. Thus a current-driven lean can cause the towfish trajectory as overlaid on Figure 8 to have any slope and any y-intercept, resulting in maxima and minima with any separation from a few metres up, or no observable maxima if the trajectory is more-or-less parallel to an interference maximum.

This model is consistent with observation, as shown by the following comparisons:

- The inter-maxima spacings observed in any particular pass which imaged all the corner cubes are similar, as the leans would be if current driven.
- The inter-maxima spacings observed in the five different passes do differ, consistent with different lean angles in different passes. Two passes show no noticeable maxima, as would tend to happen at small lean angles.
- The intensities of the principal maxima shown in Figure 6 are not equal. Two appear to be at the saturation response of the amplifiers, while the other two are far less. The differences are too large to be due to the scattering cross-section, indicating that interference is occurring.

CONCLUSIONS

This analysis has lead to three conclusions which may have an impact on future use of high-resolution sonars for bottom imaging.

- The sonar image of high reflectivity targets is affected by energy broadcast and received by the transducer at angles of up to 30°.
- The sonar trace from dual-corner-cube targets is not inconsistent with the beam pattern of the transducer, but is modulated by the interference pattern from the two sources.
- Towfish yaw can have noticeable effects on sonar images, even at short ranges.

REFERENCES

1. J.M. Preston, "Coordinates as Determined by Side-Scan Sonar - Theory and Applications", Defence Research Establishment Pacific Technical Memorandum 87-02 (1988).

2. R.G. Racca and W. Yee, "Study of Ship and Sidescan Sonar Towfish Tracking using PINS and Target Location Accuracies using Two Algorithims", Defence Research Establishment Pacific Contractor Report (Jasco Research Ltd.) (1987).

3. R.C. Spencer, "Optical Theory of the Corner Reflector", Radiation Laboratory, Massachusetts Institute of Technology, Report 433 (1944).

4. K.M. Keen, "New Technique for the Evaluation of the Scattering Cross-Sections of Radar Corner Reflectors", IEE Proc., 130, H322-326 (1983).

5. R.J. Urick, "Principles of Underwater Sound", McGraw-Hill (1975) Table 9.1.

6. A.W. Hart, "Transmit Beam Pattern Measurements on the Klein 500-kHz Side-Scan Sonar", JH Technical Memorandum 89/85, Admiralty Research Establishment Portland (1985).

7. K.M. Keen, "Prediction of Scattering Cross-Section Reductions due to Plate Orthogonality Errors in Trihedral Radar Reflectors", Elec. Lett., 19 115-117 (1983).

8. L.E. Kinsler et al, "Fundamentals of Acoustics", Third Edition, John Wiley and Sons, Chap. 8 (1982).

DISTRIBUTION LIST

"AN ANALYSIS OF SIDE-SCAN SONAR IMAGES
OF A HIGH-REFLECTIVITY TARGET"

NDHQ and Maritime Command:

3	DSIS
1	CRAD/DRDM
1	DREA
1	RRMC Library
1	DMCS-3
1	DMES-3

Internal:

5	DREP Library
1	H/Applied Technology
1	H/Magnetics
1	Group Leader, Mine Countermeasures, (Dr. R.H. Kuwahara)
1	Dr. J.M. Preston
1	Dr. W.M. Vogel
1	Dr. R.H. Poeckert

TTCP/GTP-13 and International:

1 Materials Research Laboratories
Underwater Weapons and Countermeasures Division
MRL Melbourne
P.O. Box 50, Ascot Vale
Victoria 3032, Australia
Attn: Research Leader, Mine Warfare.

1 Defence Scientific Establishment
Auckland Naval Base Post Office
Auckland New Zealand
Attn: Head MCM Group

1 Admiralty Research Establishment
Southwell, Portland, Dorset
England, DT5 2JS
Attn: Head MCM Division

1 Admiralty Research Establishment
Southwell, Portland, Dorset
England, DT5 2JS
Attn: Route Survey Group

1 Office of Naval Technology
800 N. Quincy Street
Arlington, Virginia
22217-5000
Attn: US GTP-13 National Leader

1 Naval Coastal Systems Center
Code 40C
Panama City, Florida
32407-5000
Attn: Head Minehunting Research

1 Naval Coastal Systems Center
Code 40D
Panama City, Florida
32407-5000
Attn: GTP-13 Representative

DOCUMENT CONTROL DATA

(Security classification of title, body of abstract and indexing annotation must be entered when the overall document is classified)

1. ORIGINATOR (the name and address of the organization preparing the document. Organizations for whom the document was prepared, e.g. Establishment sponsoring a contractor's report, or tasking agency, are entered in section 8.)

Defence Research Establishment Pacific
Forces Mail Office
Victoria, B.C. V0S 1B0

2. SECURITY CLASSIFICATION (overall security classification of the document including special warning terms if applicable)

UNCLASSIFIED

3. TITLE (the complete document title as indicated on the title page. Its classification should be indicated by the appropriate abbreviation (S,C,R or U) in parentheses after the title.)

ANALYSIS OF SIDE-SCAN SONAR IMAGES OF A HIGH-REFLECTIVITY TARGET.

4. AUTHORS (Last name, first name, middle initial)

Preston, Jonathan M., Poeckert, Roland H., Tribes, Michael G., and Vogel, William H.

5. DATE OF PUBLICATION (month and year of publication of document)	6a. NO. OF PAGES (total containing information. Include Annexes, Appendices, etc.)	6b. NO. OF REFS (total cited in document)
November 1988	19	8

7. DESCRIPTIVE NOTES (the category of the document, e.g. technical report, technical note or memorandum. If appropriate, enter the type of report, e.g. interim, progress, summary, annual or final. Give the inclusive dates when a specific reporting period is covered.)

DREP TECHNICAL MEMORANDUM

8. SPONSORING ACTIVITY (the name of the department project office or laboratory sponsoring the research and development. Include the address.)

9a. PROJECT OR GRANT NO. (if appropriate, the applicable research and development project or grant number under which the document was written. Please specify whether project or grant)	9b. CONTRACT NO. (if appropriate, the applicable number under which the document was written)

10a. ORIGINATOR'S DOCUMENT NUMBER (the official document number by which the document is identified by the originating activity. This number must be unique to this document.)	10b. OTHER DOCUMENT NOS. (Any other numbers which may be assigned this document either by the originator or by the sponsor)
TM 88-26	

11. DOCUMENT AVAILABILITY (any limitations on further dissemination of the document, other than those imposed by security classification)

( ) Unlimited distribution
(XX) Distribution limited to defence departments and defence contractors; further distribution only as approved
( ) Distribution limited to defence departments and Canadian defence contractors; further distribution only as approved
( ) Distribution limited to government departments and agencies; further distribution only as approved
( ) Distribution limited to defence departments; further distribution only as approved
( ) Other (please specify):

12. DOCUMENT ANNOUNCEMENT (any limitation to the bibliographic announcement of this document. This will normally correspond to the Document Availabilty (11). However, where further distribution (beyond the audience specified in 11) is possible, a wider announcement audience may be selected.)

13. ABSTRACT (a brief and factual summary of the document. It may also appear elsewhere in the body of the document itself. It is highly desirable that the abstract of classified documents be unclassified. Each paragraph of the abstract shall begin with an indication of the security classification of the information in the paragraph (unless the document itself is unclassified) represented as (S), (C), (R), or (U). It is not necessary to include here abstracts in both offical languages unless the text is bilingual).

An investigation of the image produced by a commercial side-scan sonar operating against moored reflectors is reported. This study of reflections from triangular corner cubes showed that energy broadcast and received at angles of up to 30° can appear on the image of high reflectivity targets, even with sonars of nominal beamwidths of less than 1°. This unusual image was found to be consistent with the beam pattern of the transducer. An effect of towfish yaw could also be seen in the image studied.

14. KEYWORDS, DESCRIPTORS or IDENTIFIERS (technically meaningful terms or short phrases that characterize a document and could be helpful in cataloguing the document. They should be selected so that no security classification is required. Identifiers, such as equipment model designation, trade name, military project code name, geographic location may also be included. If possible keywords should be selected from a published thesaurus. e.g. Thesaurus of Engineering and Scientific Terms (TEST) and that thesaurus-identified. If it is not possible to select indexing terms which are Unclassified, the classification of each should be indicated as with the title.)

Sonar
Sidescan Sonar
Side Scan Sonars
Corner Reflectors
Triangular Reflectors